High-pressure structural study of fluoro-perovskite CsCdF$_3$ up to 60 GPa: A combined experimental and theoretical study

G. Vaitheeswaran,[1,2,*] V. Kanchana,[1] Ravhi S. Kumar,[3] A. L. Cornelius,[3] M. F. Nicol,[3,4] A. Svane,[5] N. E. Christensen,[5] and O. Eriksson[6]

[1]*Applied Materials Physics, Department of Materials Science and Engineering, Royal Institute of Technology, Brinellvägen 23, 100 44 Stockholm, Sweden*

[2]*Advanced Centre of Research in High Energy Materials (ACRHEM), University of Hyderabad, Hyderabad 500 046, Andhra Pradesh, India*

[3]*High Pressure Science and Engineering Center and Department of Physics, University of Nevada, Las Vegas, Nevada 89154, USA*

[4]*Department of Chemistry, University of Nevada, Las Vegas, Nevada 89154, USA*

[5]*Department of Physics and Astronomy, Aarhus University, DK-8000 Aarhus C, Denmark*

[6]*Department of Physics and Materials Science, Uppsala University, P.O. Box 590, SE-751 21 Uppsala, Sweden*

The structural behavior of CsCdF$_3$ under pressure is investigated by means of theory and experiment. High-pressure powder x-ray diffraction experiments were performed up to a maximum pressure of 60 GPa using synchrotron radiation. The cubic $Pm\bar{3}m$ crystal symmetry persists throughout this pressure range. Electronic structure calculations were carried out using the full-potential linear muffin-tin orbital method within the local-density approximation and the generalized gradient approximation for exchange and correlation effects. The calculated ground-state properties—the equilibrium lattice constant, bulk modulus and elastic constants—are in good agreement with experimental results. The calculations reveal that CsCdF$_3$ is an indirect-gap insulator under ambient conditions, with the gap increasing under pressure.

I. INTRODUCTION

Ternary fluorides with the perovskite crystal structure have been extensively studied over several decades, as they have many potential applications due to their optical properties,[1–3] high-temperature superionic behavior,[4] ferroelectricity,[5] antiferromagnetism,[6] and semiconductivity.[7] Perovskite fluorides may or may not exhibit structural phase transitions as function of temperature and pressure,[8–18] and the present work investigates the structural properties of the CsCdF$_3$ compound under pressure by both experiment and theory.

The application of CsCdF$_3$ in the field of luminescence[19–21] has motivated several experimental and theoretical investigations of defect structures involving 3d transition-metal ions.[22–30] Studies of lattice thermal expansion and elastic properties, including acoustical measurements of higher order elastic constants, have been reported.[12–15,31] The thermal expansion and temperature dependent structural experiments on CsCdF$_3$ reported by Reddy *et al.*,[14] in the temperature range of 20–450 °C showed that the coefficient of thermal expansion increases smoothly with temperature without any signs of structural transitions. Rousseau *et al.*[12] investigated the crystal structure and elastic constants of RbCdF$_3$, TlCdF$_3$, and CsCdF$_3$ using x-ray diffraction and Raman techniques at temperatures from 4 K to room temperature. They found tetragonal distortions in RbCdF$_3$ and TlCdF$_3$ at 124 and 191 K, respectively. However, no structural phase transition was found for CsCdF$_3$ in the temperature range studied. Investigations by Haussuhl[32] have found that temperature induced transitions can be observed in the pseudocubic perovskite CsCd(NO$_2$)$_3$, which undergoes a phase transition from $R3$ to $Pm3m$ sym-

metry around 464 K.[32] These reports indicate that the cubic structure of CsCdF$_3$ is relatively stable in comparison with RbCdF$_3$ and TlCdF$_3$ for a wide range of temperature from 4 to 750 K.

The pressure dependence of the second-order elastic constants of CsCdF$_3$ and related fluoro-perovskites were investigated by Refs. 13 and 15. These authors reported a decrease in the force constants in RbCdF$_3$ and TlCdF$_3$, which is connected with the instability of the F ions. Such instability has not been noticed for CsCdF$_3$, however a possible phase transition at high pressure was suggested based on the strong second-order pressure variation of the C_{44} elastic constant.[15] So far, no high-pressure experiments have been reported to elucidate the structural behavior of CsCdF$_3$. In a previous work we investigated the fluoro-perovskite KMgF$_3$, which was found to remain cubic under pressure up to 40 GPa.[11] If any structural phase transition is to be induced in CsCdF$_3$, one would expect that pressures above 40 GPa are required. However, the diffraction patterns collected in our experiments show no pressure induced structural transformations up to 60 GPa. That is, similarly to KMgF$_3$, the cubic phase of CsCdF$_3$ remains stable up to the highest pressures achieved in our experiments.

The remainder of the paper is organized as follows. Section II introduces briefly the computational method, which is based on density functional theory, and provides details of the experimental high-pressure diamond-anvil setup. The measured and calculated pressure-volume relations are presented in Sec. III together with calculated structural and elastic properties at ambient pressure. The theoretical results regarding the electronic structure of CsCdF$_3$ and the pressure variation of the band gap are discussed in Sec. IV. Finally, conclusions are given in Sec. V.
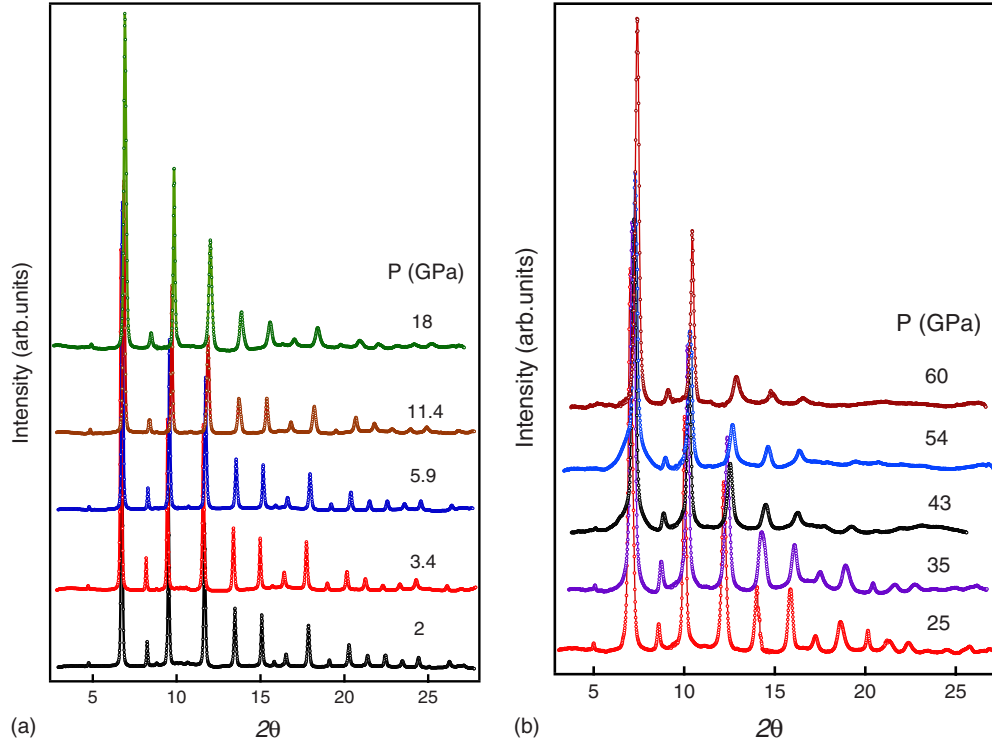
FIG. 1. (Color online) Powder x-ray diffraction patterns of CsCdF₃ recorded at (a) pressures below 25 GPa and (b) pressures above 25 up to 60 GPa.

II. COMPUTATIONAL AND EXPERIMENTAL DETAILS

A. Electronic structure method

The total energies and basic ground-state properties of CsCdF$_3$ were calculated by the all-electron linear muffin-tin orbital (LMTO) method[33] in the full-potential implementation of Ref. 34. In this method, the crystal volume is split into two regions: nonoverlapping muffin-tin spheres surrounding each atom and the interstitial region between these spheres. We used a double κ spdf LMTO basis to describe the valence bands, *i.e.*, atom-centered Hankel functions with characteristic decay rate denoted by κ are matched to a linear combination of products of numerical radial function and spherical harmonics within the muffin-tin spheres. The calculations included the $5s$, $5p$, $6s$, and $5d$ partial waves for cesium, the $5s$, $5p$, and $4d$ partial waves for cadmium, and the $2s$ and $2p$ partial waves for fluorine. The exchange-correlation potential was calculated within the local-density approximation (LDA) (Ref. 35) as well as the generalized gradient approximation (GGA) scheme.[36] The charge density and potential inside the muffin-tin spheres were expanded in terms of spherical harmonics up to $l_{max}=6$, while in the interstitial region, they were expanded in plane waves, with 14146 waves (energy up to 156 Ry) included in the calculation. Total energies were calculated as a function of volume for a (16 16 16) k mesh containing 165 k points in the irreducible wedge of the Brillouin zone and were fitted to a second-order Birch-Murnaghan equation of state[37] to obtain the theoretical equilibrium volume, bulk modulus and bulk modulus derivative. The elastic constants were obtained from the variation of the total energy under volume-conserving strains, as outlined in Refs. 38 and 39.

B. Experimental details

Polycrystalline samples of CsCdF₃ were synthesized by the solid-state reaction method as described elsewhere.[4,17,40] For high-pressure powder-diffraction experiments, samples with a few ruby chips were loaded in a Mao-Bell-type diamond-anvil cell in a rhenium gasket (135 μm hole diameter and preindentation thickness 65 μm). Pressure was generated with 325 μm culet diamonds. Silicone fluid was used as the pressure transmitting medium.[41] The silicone fluid behaves very similar to a 4:1 methanol-ethanol mixture at pressures below 20 GPa, and above 20 GPa it is superior to the methanol-ethanol mixture and comparable to Ar.[42] X-ray diffraction experiments were performed at Sector 16 ID-B, HP-CAT, at the Advanced Photon Source. The pressure inside the
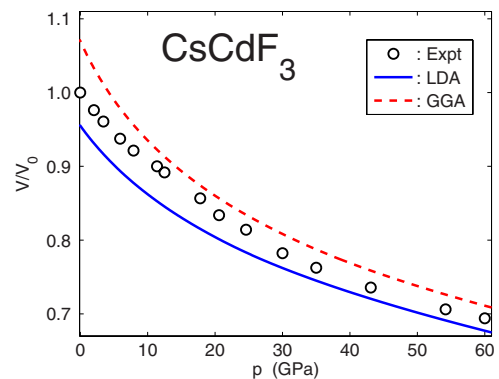

FIG. 2. (Color online) Measured (circles) and calculated (full line: LDA; broken line: GGA) pV relation of CsCdF₃. V_0 is the experimental equilibrium volume, $V_0=89.13$ Å³.

TABLE I. Lattice constants (in Å), bulk modulus B_0 (in GPa) and its pressure derivative B_0', of $CsCdF_3$ as obtained by experiment and theory. The bulk moduli have been calculated both at the experimental and theoretical volumes [$B_0(V_0^{exp})$ and $B_0(V_0^{th})$, respectively].

	Lattice constant	$B_0(V_0^{th})$	$B_0(V_0^{exp})$	B_0'
GGA[a]	4.567	53.3	73.6	4.9
LDA[a]	4.397	75.6	59.7	4.9
Expt. (RT)	4.4669(7)[a],4.465[b],4.4662[c],		79(3)[a]	3.8[a],5.8[d]
Expt.($T=0$ K)	4.452[b]			

[a]Present work
[b]Reference 12.
[c]Reference 14.
[d]Reference 15.

diamond-anvil cell was determined by the standard ruby luminescence method.[43] The incident monochromatic x-ray wavelength was $\lambda=0.36798$ Å. The x-ray diffraction patterns were recorded on an imaging plate with a typical exposure time of 10–20 s, with an incident-beam size of 20×20 μm. The distance between the sample and the detector was calibrated using a CeO_2 standard. The patterns were integrated using the FIT2D software program[44] and the cell parameters were obtained using the JADE package.

The evolution of diffraction patterns as a function of pressure is shown in Fig. 1. At ambient conditions the cell parameter a=4.4669(7) Å obtained experimentally agrees well with earlier reports provided in the inorganic crystal structure database (ICSD).[45] The corresponding experimental equilibrium volume is $V_0^{exp}=89.13$ Å^3.

The bulk modulus was obtained by fitting the pressure-volume data to a second-order Birch-Murnaghan equation of state,[37]

$$P = \frac{3}{2}B_0[(V/V_0)^{-7/3} - (V/V_0)^{-5/3}]\{1 + 3/4(B_0' - 4)$$
$$\times[(V/V_0)^{-2/3} - 1]\}, \quad (1)$$

where V_0 is the equilibrium volume at zero pressure, B_0 is the bulk modulus and B_0' its pressure derivative. Least square fitting with $V_0=V_0^{exp}$ resulted in a B_0 of 79(3) GPa, with a B_0' of 3.8. Thus, $CsCdF_3$ has a slightly higher bulk modulus than $KMgF_3$ ($B_0=71.2$ GPa, $B_0'=4.7$).[11]

III. STRUCTURAL AND ELASTIC PROPERTIES

Powder x-ray diffraction patterns collected at several pressures are shown in Figs. 1(a) and 1(b). In Fig. 1(a) the diffraction peaks collected below 25 GPa are shown explicitly, while Fig. 1(b) shows the diffraction peaks collected from 25 to 60 GPa. On compression, the diffraction patterns remain unchanged up to 60 GPa except for the shifts of diffraction lines caused by the decreasing lattice constant and the broadening due to the internal strains in the sample at elevated pressures. This implies that no structural transformations occur up to 60 GPa in $CsCdF_3$. Figure 2 shows the compression curve of $CsCdF_3$ and compares it with theoretical curves calculated within the LDA and GGA. As is typical, the LDA leads to slightly smaller crystal volume at a

given pressure than the experiment, while the GGA gives a larger crystal volume compared to experiment.

The lattice constant and bulk modulus (at ambient conditions) measured in the present work, as well as values calculated within the LDA and GGA are given in Table I. Results from earlier experimental works are also quoted for comparison. The bulk modulus obtained in our experiments B_0 =79(3) GPa with B_0'=3.8, compares well with values calculated using the LDA. The lattice constant obtained within the LDA is 1.6% lower than the experimental value, while the corresponding bulk modulus is 4.7% lower than the experimental value, which is the usual level of accuracy of the LDA. When comparing the results obtained within GGA, the lattice constant is 2.2% higher than the experimental value and the corresponding bulk modulus is 32% lower than the experimental value. Since the present theory does not describe thermal effects, it is more relevant to compare to the low-temperature experimental lattice constant, which is 0.4% lower than the room-temperature (RT) value (Table I). Further, taking the zero-point motion of the ions into account, an even better agreement between LDA theory and experiment is obtained. Hence, it is safe to conclude that the LDA lattice constant is in fact in better agreement with the experimental lattice constant than the GGA value. The same conclusion was reached for the $KMgF_3$ compound.[11] The excellent agreement between the LDA calculated bulk modulus and the experimental value is, however, fortuitous, since the bulk modulus depends strongly on volume. Due to the overestimated equilibrium volume within GGA (and underestimated with LDA), an error is introduced in the calculated bulk modulus. Therefore, we recalculated the bulk modulus also at the experimental volume, using the derived Birch-Murnaghan equation of state. The corrected values are also

TABLE II. Calculated elastic constants and shear modulus (G), all expressed in GPa, of $CsCdF_3$ at the theoretical equilibrium volume.

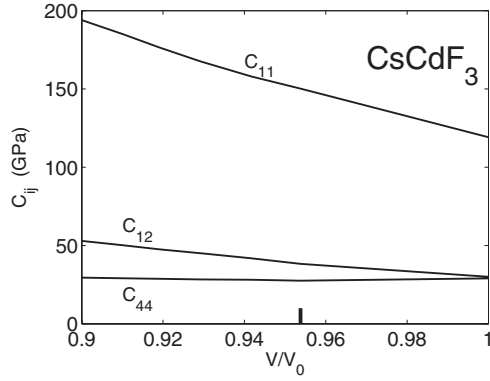|	C_{11}	C_{12}	C_{44}	G	
GGA	105.8	27.0	27.7	32.4	Present
LDA	150.2	38.3	27.5	38.9	Present
Expt.	107.8±0.2	40.5±0.5	25.0±0.2	28.5±0.5	Ref. 12

FIG. 3. Volume variation of the elastic constants of $CsCdF_3$ as calculated in LDA. The volume is given relatively to the experimental equilibrium volume, V_0 (see Sec. II), while the theoretical LDA equilibrium volume is marked with a vertical bar on the first axis.

TABLE III. Calculated LDA pressure derivatives of the elastic constants of $CsCdF_3$ at the experimental equilibrium volume.

	$\frac{dC_{11}}{dp}$	$\frac{dC_{12}}{dp}$	$\frac{dC_{44}}{dp}$	
LDA	8.8	2.9	0.4	Present
Expt.	11.1 ± 0.1	3.2 ± 0.1	2.2 ± 0.4	Ref. 15

quoted in Table I. We find that this diminishes the discrepancies between the LDA and GGA results, as expected. In addition, the LDA bulk modulus now becomes *smaller* than the GGA one for $CsCdF_3$, and both functionals are seen to actually underestimate the bulk modulus, by approximately 25% (LDA) and 7% (GGA).

The elastic constants of $CsCdF_3$ calculated within LDA and GGA are listed in Table II where they are also compared to experimental results as well as earlier calculations. The LDA overestimates the C_{11} value by 28% and the corresponding GGA value is 1.8% lower than the experimental value. The C_{12} value within LDA is 5.4% lower than the experiment, and the corresponding GGA value is 33.3% higher than the experiment. The C_{44} elastic constants are higher by 9% both within LDA and GGA compared to experiment.[12] The C_{11} elastic constant obtained within GGA is much closer to the experimental value than the LDA value, while for C_{12} the situation is reversed, and for C_{44} the two approaches give approximately the same value, and in reasonable agreement with the experimental value. The elastic constants depend sensitively on the volume as illustrated in Fig. 3 for the case of LDA. Hence the above values carry an appreciable uncertainty inherited from the volume inaccuracy of the LDA or GGA approach. The pressure derivatives

of the elastic constants are more stable quantities. They are compared to experimental values[15] in Table III with a reasonable agreement. The C_{11} has the strongest pressure dependence in accordance with the experiment, while the theoretical C_{44} value is almost constant with pressure, while experiment find it increasing with pressure. A point of caution is the fact that the present theory pertains to $T=0$ K, while experiments are performed at room temperature. Finite temperature generally tends to reduce the elastic constants because of thermal expansion (reducing interatomic force constants), as also found experimentally for $CsCdF_3$.[13,15] Using the calculated elastic constants we calculated the anisotropy factor $A=2C_{44}/(C_{11}-C_{12})$. We find an $A=0.49$ for LDA and $A=0.70$ for GGA. The experimental[12] value calculated from the elastic constants is 0.74 which is slightly higher than the GGA value.

IV. ELECTRONIC STRUCTURE

The calculated electron band structure of $CsCdF_3$ is shown in Fig. 4, at two volumes corresponding to $p=0$ GPa and $p=60$ GPa, respectively. The density of states corresponding to ambient conditions is displayed in Fig. 5. The valence bands consist of the fluorine p bands, which dominate the first 2 eV below the valence-band maximum. Below these bands appear the Cs $5p$ bands and the Cd $4d$ bands, which hybridize heavily in the region from 6 to 4 eV below the top of the valence band. The Cd $5s$ and Cs $6s$ states dominate the bottom of the conduction band. The insulating gap is calculated to be 3.16 eV in LDA (3.67 eV in GGA). The gap increases with pressure, with the deformation potential given as
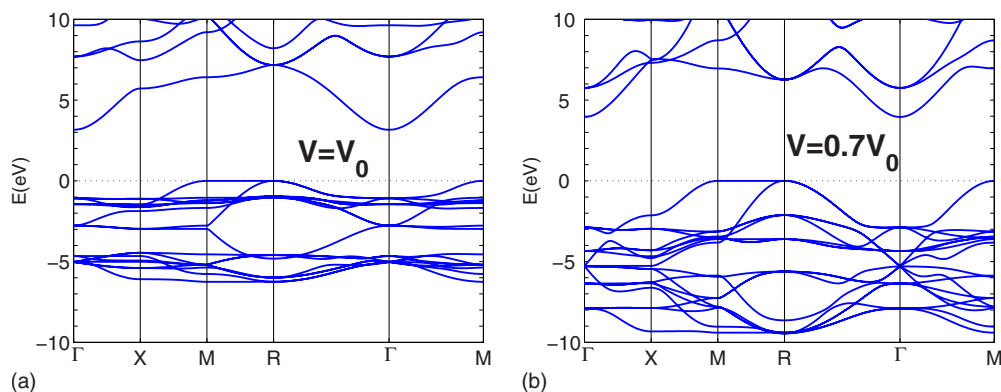

FIG. 4. (Color online) Band structure of $CsCdF_3$ (using LDA). (a): at the experimental lattice constant, $a=4.4669$ Å; (b): at compression corresponding to $p=60$ GPa and $a=3.969$ Å. The zero of energy is set at the position of the valence-band maximum at the R point.
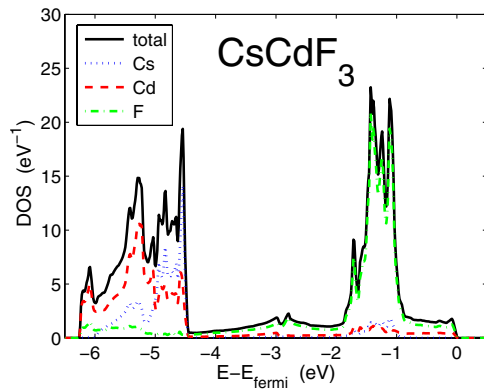
FIG. 5. (Color online) Valence-band density of states of $CsCdF_3$ (using LDA, at the experimental lattice constant). The zero of energy is set at the position of the valence-band maximum. The partial projections onto the spheres of Cs, Cd and F are shown with dotted (blue), dashed (red) and dash-dotted (green) lines, respectively, while the full line gives the total density of states. Units are electrons per eV and per formula unit.

$$V\frac{dE_g}{dV} = -2.1 \ \text{eV}.$$

On the one hand pressure leads to band broadening which would cause band gaps to diminish, but on the other hand pressure also increases the splitting between the F $2p$ level, and the Cs $6s$- and Cd $5s$-levels. For $CsCdF_3$, the latter effect is largest and explains the increasing fundamental gap under pressure. The conduction-band minimum occurs at the Γ point, while the valence-band maximum occurs at the R-point $(1/2,1/2,1/2)\frac{2\pi}{a}$, however almost no dispersion is found for the uppermost valence band along the line connecting the R point with the M point $(1/2,1/2,0)\frac{2\pi}{a}$. This topol-

ogy of the band structure remains throughout the pressure range studied here, $p < 60$ GPa. At $p = 60$ GPa ($V/V_0 \sim 0.7$) the minimum gap has increased to 3.96 eV (LDA). The valence-band width at the same time has increased from 6.2 eV at $p = 0$ to 9.4 eV at $p = 60$ GPa.

V. CONCLUSIONS

In the present work, a combined theoretical and experimental analysis of the structural stability and pressure-volume relation of the fluoro-perovskite $CsCdF_3$ has been carried out up to a pressure of 60 GPa. We find that the compound remains in the cubic structure in the entire pressure range studied. The calculated equilibrium lattice constant, bulk modulus and elastic constants agree well with available experimental data. The electronic structure calculations show that $CsCdF_3$ is an insulator with an indirect gap which increases with pressure.

*Corresponding author; vaithee@kth.se

[1] G. Hörsch and H. J. Paus, Opt. Commun. **60**, 69 (1986).

[2] R. Hua, B. Lei, D. Xie, and C. Shi, J. Solid State Chem. **175**, 284 (2003).

[3] K. Shimamura, H. Sato, A. Bensalah, V. Sudesh, H. Machida, N. Sarukura, and T. Fukuda, Cryst. Res. Technol. **36**, 801 (2001).

[4] A. V. Chadwick, J. H. Strange, G. A. Ranieri, and M. Terenzi, Solid State Ionics **9-10**, 555 (1983).

[5] P. Berastegui, S. Hull, and S.-G. Eriksson, J. Phys.: Condens. Matter **13**, 5077 (2001).

[6] J. Julliard and J. Nouet, Rev. Phys. Appl. **10**, 325 (1975).

[7] R. R. Daniels, G. Margaritondo, R. A. Heaton, and C. C. Lin, Phys. Rev. B **27**, 3878 (1983).

[8] N. Lehner, H. Rauh, K. Strobe, R. Geick, G. Heger, J. Bouillot, B. Renker, M. Rousseau, and W. G. Stirling, J. Phys. C **15**, 6545 (1982).

[9] S. Åsbrink, A. Waskowska, H. G. Krane, L. Gerward, and J. S. Olsen, J. Appl. Crystallogr. **32**, 174 (1999).

[10] E. K. H. Salje, M. Zhang, and H. Zhang, J. Phys.: Condens. Matter **21**, 335402 (2009).

[11] G. Vaitheeswaran, V. Kanchana, S. Ravhi Kumar, A. L. Cornelius, M. F. Nicol, A. Svane, A. Delin, and B. Johansson, Phys. Rev. B **76**, 014107 (2007).

[12] M. Rousseau, J. Y. Gesland, J. Julliard, J. Nouet, J. Zarembowitch, and A. Zarembowitch, Phys. Rev. B **12**, 1579 (1975).

[13] A. Zarembowitch, B. Perrin, and M. Fischer, J. Phys. Colloq. **40**, C8-168 (1979).

[14] K. D. Reddy, P. Kistaiah, and L. Iyengar, J. Less-Common Met. **92**, 81 (1983).

[15] M. Fischer, J. Phys. Chem. Solids **43**, 673 (1982).

[16] Y. S. Zhao, J. B. Parise, Y. B. Wang, K. Kusaba, M. T. Vaughan, D. J. Weidner, T. Kikegawa, J. Chen, and O. Shimomura, Am. Mineral. **79**, 615 (1994).

[17] Y. S. Zhao, J. Solid State Chem. **141**, 121 (1998).

[18] A. R. Chakhmouradian, K. Ross, R. H. Mitchell, and I. Swainson, Phys. Chem. Miner. **28**, 277 (2001).

[19] B. Villacampa, R. Cases, V. M. Orera, and R. Alcala, J. Phys. Chem. Solids **55**, 263 (1994).

[20] B. Villacampa, R. Cases and R. Alcala, J. Lumin. **63**, 289 (1995).

[21] M. T. Barriuso, M. Moreno, and J. A. Aramburu, Phys. Rev. B **65**, 064441 (2002).

[22] M. E. Ziaei and J. Owen, J. Phys. C **9**, L529 (1976).

[23] C. D. Adam, A. H. Harker, and J. Owen, J. Phys. C **12**, L239 (1979).

[24] E. Minner, D. Lovy, and H. Bill, J. Chem. Phys. **99**, 6378 (1993).

[25] M. Springis, A. Sharakovsky, I. Tale, and U. Rogulis, Phys. Status Solid C **2**, 511 (2005).

[26] H. Takeuchi, M. Arakawa, and H. Ebisu, J. Phys. Soc. Jpn. **56**, 3677 (1987).

[27] J. S. Yao, S. Y. Wu, X. Y. Gao, and H. M. Zhang, Hyperfine Interact. **174**, 103 (2007).

[28] J.-H. Li, X.-Y. Kuang, M.-L. Duan, and Z.-Y. Jiao, Solid State Commun. **141**, 279 (2007).

[29] S. Y. Wu, Z. H. Zhang, L. H. Wei, H. Wang, and Y. X. Hu, Chem. Phys. **348**, 199 (2008).

[30] J. A. Aramburu, J. I. Paredes, M. T. Barriuso, and M. Moreno, Phys. Rev. B **61**, 6525 (2000).

[31] M. A. Breazeale, J. Philip, A. Zarembowitch, M. Fischer, and Y. Gesland, J. Sound Vib. **88**, 133 (1983).

[32] S. Haussuhl, Cryst. Res. Technol. **29**, 697 (1994).

[33] O. K. Andersen, Phys. Rev. B **12**, 3060 (1975).

[34] S. Y. Savrasov, Phys. Rev. B **54**, 16470 (1996).

[35] S. H. Vosko, L. Wilk, and M. Nusair, Can. J. Phys. **58**, 1200 (1980).

[36] J. P. Perdew, K. Burke, and M. Ernzerhof, Phys. Rev. Lett. **77**, 3865 (1996). We use the proposed value $\kappa = 0.804$ in the gradient enhancement factor of this functional.

[37] F. Birch, Phys. Rev. **71**, 809 (1947).

[38] V. Kanchana, G. Vaitheeswaran, A. Svane, and A. Delin, J. Phys.: Condens. Matter **18**, 9615 (2006).

[39] V. Kanchana, G. Vaitheeswaran, and A. Svane, J. Alloys Compd. **455**, 480 (2008).

[40] R. W. Smith, W. N. Mei, J. W. Flocken, M. J. Dudik, and J. R. Hardy, Mater. Res. Bull. **35**, 341 (2000).

[41] Y. R. Shen, R. S. Kumar, M. Pravica, and M. F. Nicol, Rev. Sci. Instrum. **75**, 4450 (2004).

[42] S. Klotz, J.-C. Chervin, P. Munsch, and G. Le Marchand, J. Phys. D **42**, 075413 (2009).

[43] H. K. Mao, J. Xu, and P. M. Bell, J. Geophys. Res. **91**, 4673 (1986).

[44] A. P. Hammersley, S. O. Svensson, M. Hanfland, A. N. Fitch, and D. Häusermann, High Press. Res. **14**, 235 (1996).

[45] C. Q. Wu and R. Hoppe, Z. Anorg. Allg. Chem. **514**, 92 (1984).